

**METHOD OF CONTROL OF A STRAKED WING AIRCRAFT FOR COBRA MANOEUVRES**

Zbigniew Dzygadlo\*, Grzegorz Kowaleczko\*\*, Krzysztof Sibilski\*\*\*  
 Military University of Technology  
 and Aviation Institute  
 Warsaw, Poland

Abstract

Dynamics of spatial motion of a supersonic combat aircraft with a straked wing is considered for post stall manoeuvres. A method of the aircraft control is proposed which enables to perform a deep stall manoeuvre called Cobra. Computational modelling of the motion is carried out by way of example of the MiG-29 aircraft.

Aerodynamic characteristics of that aircraft have been determined making use of the results of wing tunnel investigations and theoretical calculations. Deep stall characteristics of the aircraft have also been found.

Computer modelling of Cobra manoeuvres performed by MiG-29 aircraft have been investigated for various initial data. Results of numerical analysis show the effect of the law of control and initial data on the course of flight parameters during Cobra manoeuvres.

Limit cases in which that manoeuvre can still be realised are determined.

Nomenclature

- V - aircraft air velocity
- F - thrust
- m - aircraft mass
- $I_x, I_y, I_z, I_{xz}$  - aircraft moments of inertia
- g - acceleration of gravity
- $P_{xa}, P_{ya}, P_{za}$  - components of aerodynamic forces in the velocity co-ordinates
- $L_C, M_C, N_C$  - components of the moment of forces in the body-fixed axes
- $\alpha, \beta$  - angles of attack and sideslip
- $p, q, r$  - components of the angular rate vector in the body-fixed axes
- $\Theta, \Phi, \Psi$  - angles of pitch, roll and yaw
- $\varphi$  - angle of engines setting
- t - time
- S - wing area
- $\rho$  - air density
- $l_a$  - mean aerodynamic chord
- l - wingspan

\* Prof. D. Sc. Eng.  
 \*\* D. Sc. Eng. \*\*\* D. Sc. Eng.

1. Introduction

Cobra is an aircraft manoeuvre which is performed with very high instantaneous angles of attack, of the order of  $90^\circ$  or so, and returning to level flight in a matter of seconds, without any appreciable change in altitude. It was executed by MiG-29 and Su-27 fighters. An analysis performed last years showed that several other aircraft would be capable of executing similar manoeuvres (cf. [1]-[4]).

In this paper spatial motion of a supersonic combat aircraft with a straked wing is investigated for post stall manoeuvres and computational modelling of the motion dynamics is carried out by way of example of the MiG-29 aircraft.

Aerodynamic characteristics of that aircraft have been obtained by means of the wind tunnel model investigations and theoretical calculations. Post stall characteristics of the aircraft have also been determined.

A method of the aircraft control is proposed which enables to perform a deep stall Cobra manoeuvre. Computer modelling of this manoeuvre executed by the MiG-29 aircraft have been studied for various initial data.

The equations of motion of the centre of mass of the aircraft have been written in the air-trajectory reference frame and equations of moments - in the body-fixed axes. The effect of gyroscopic moments of the engine rotors on the dynamics of motion of the aircraft can be taken into account [5]-[7].

2. Equations of the Problem

Let us consider an aircraft spatial motion. The equations of its motion and kinematic relations will be expressed making use of moving co-ordinate systems, the common origin of which is located at the centre of mass of the aircraft (Figs. 1 and 2).

We shall apply a vertical moving system of co-ordinates  $Ox_g y_g z_g$ , the  $Oz_g$  axis of which is vertical and directed downwards, a system of co-ordinates  $Oxyz$  attached to the aircraft (body axes), where the  $Oxz$  plane coincides with the symmetry plane of the aircraft, and a system  $Ox_a y_a z_a$  attached to the air trajectory

(velocity axes), in which the  $Ox_a$  axis is directed along the flight velocity vector  $V$  and the  $Oz_a$  axis lies in the symmetry plane of the aircraft directed downwards.

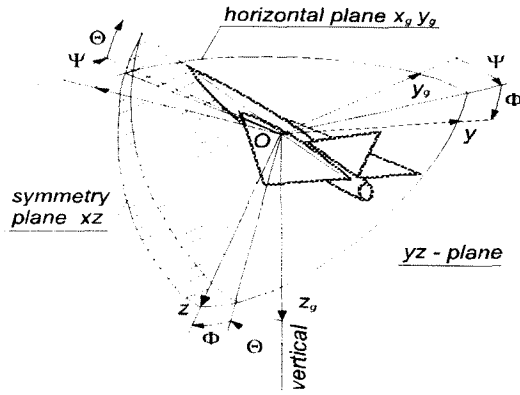


Figure 1

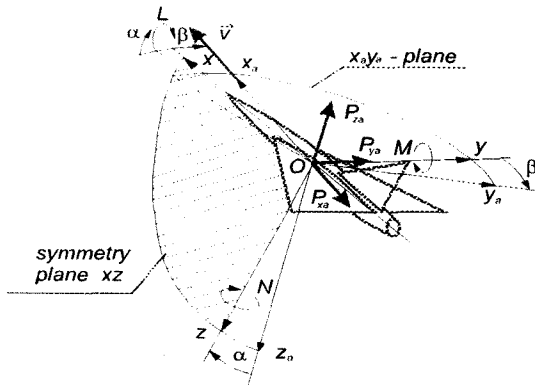


Figure 2

The relative position of the vertical system  $Ox_a y_a z_a$  and the body system  $Oxyz$ , attached to the aircraft is described by Euler angles  $\Theta$ ,  $\Phi$  and  $\Psi$  (Fig. 1), while the relative position of the system  $Oxyz$  and the system  $Ox_a y_a z_a$  attached to the air trajectory - by the angle of attack  $\alpha$  and the angle of sideslip  $\beta$  (Fig.2).

The equations of motion of the centre of mass in the velocity system of co-ordinates can be obtained in the following form (cf. [5]-[7]):

$$\begin{aligned} \dot{V} &= \frac{1}{m} \left\{ F \cos(\alpha + \varphi) - mg(\sin \Theta \cos \alpha + \right. \\ &\quad \left. - \cos \Theta \cos \Phi \sin \alpha) \right\} \cos \beta + \\ &\quad \left. + mg \cos \Theta \sin \Phi \sin \beta - P_{x_a} \right\} \\ \dot{\alpha} &= q - (p \cos \alpha + r \sin \alpha) \tan \beta + \\ &\quad - \frac{1}{mV \cos \beta} \left[ F \sin(\alpha + \varphi) - mg(\sin \Theta \sin \alpha + \right. \\ &\quad \left. - \cos \Theta \cos \Phi \cos \alpha) - P_{z_a} \right] \\ \dot{\beta} &= p \sin \alpha - r \cos \alpha - \frac{1}{mV} \left\{ F \cos(\alpha + \varphi) + \right. \\ &\quad \left. - mg(\sin \Theta \cos \alpha - \cos \Theta \cos \Phi \sin \alpha) \right\} \sin \beta + \\ &\quad \left. - mg \cos \Theta \sin \Phi \cos \beta - P_{y_a} \right\} \end{aligned} \quad (2.1)$$

The set of equations of the rotating motion about the centre of mass in the body-fixed reference frame is:

$$\begin{aligned} I_x \dot{p} + (I_z - I_y)qr - I_{xz}(\dot{r} + pq) &= L_C \\ I_y \dot{q} + (I_x - I_z)pr + I_{xz}(p^2 - r^2) &= M_C \\ I_z \dot{r} + (I_y - I_x)pq - I_{xz}(\dot{p} - qr) &= N_C \end{aligned} \quad (2.2)$$

The equations of motion (2.1), (2.2) should be completed by the following kinematic relations which enable us to determine the angular position of the aircraft with reference to the system of co-ordinates  $Ox_a y_a z_a$  (Fig.1).

$$\begin{aligned} \dot{\Psi} &= (r \cos \Phi + q \sin \Phi) / \cos \Theta \\ \dot{\Theta} &= q \cos \Phi - r \sin \Phi \\ \dot{\Phi} &= p + (q \sin \Phi + r \cos \Phi) \tan \Theta \end{aligned} \quad (2.3)$$

and the relations for determining the position of the centre of mass in the fixed coordinates:

$$\begin{aligned} \dot{x}_g &= u \cos \Theta \cos \Psi + \\ &\quad + v(\sin \Theta \sin \Phi \cos \Psi - \cos \Phi \sin \Psi) + \\ &\quad + w(\sin \Theta \cos \Phi \cos \Psi + \sin \Phi \sin \Psi) \\ \dot{y}_g &= u \cos \Theta \sin \Psi + \\ &\quad + v(\sin \Theta \sin \Phi \sin \Psi + \cos \Phi \cos \Psi) + \\ &\quad + w(\sin \Theta \cos \Phi \sin \Psi - \sin \Phi \cos \Psi) \\ \dot{z}_g &= -u \sin \Theta + v \cos \Theta \sin \Phi + \\ &\quad + w \cos \Theta \cos \Phi \end{aligned} \quad (2.4)$$

The velocity components in the reference frame attached to the aircraft can be found from the equations (Fig.2):

$$\begin{aligned} u &= V \cos \alpha \cos \beta \\ v &= V \sin \beta \\ w &= V \sin \alpha \cos \beta \end{aligned} \quad (2.5)$$

The aerodynamic forces in the velocity co-ordinates can be expressed in the form:

$$\begin{aligned} P_{x_a} &= \frac{1}{2} \rho V^2 S C_D \\ P_{y_a} &= \frac{1}{2} \rho V^2 S C_y \\ P_{z_a} &= \frac{1}{2} \rho V^2 S C_L \end{aligned} \quad (2.6)$$

and the components of the moment of forces in the right-hand members of Eqs (2.2) are:

$$\begin{aligned} L_C &= L + L_F + L_G \\ M_C &= M + M_F + M_G \\ N_C &= N + N_F + N_G \end{aligned} \quad (2.7)$$

where  $L_F$ ,  $M_F$ ,  $N_F$  are components of the engine thrust moment,  $L_G$ ,  $M_G$ ,  $N_G$  are components of the gyroscopic moment of the rotating masses of the power plant and  $L$ ,  $M$ ,  $N$  are the roll, pitch and yaw components of the aerodynamic moment of the aircraft:

$$\begin{aligned}
L &= \frac{1}{2} \rho V^2 S C_l \\
M &= \frac{1}{2} \rho V^2 S l_a C_m \\
N &= \frac{1}{2} \rho V^2 S C_n
\end{aligned} \quad (2.8)$$

Coefficients of the aerodynamic forces - that is the coefficient of drag  $C_D$ , the coefficient of lateral force  $C_y$ , the coefficient of lift  $C_L$ , and coefficients of the aerodynamic moments - the rolling moment coefficient  $C_l$ , the pitching moment coefficient  $C_m$ , the yawing moment coefficient  $C_n$  and their derivatives have been determined for the MiG-29 aircraft making use of the results of wind tunnel model investigations and theoretical calculations [5]. Deep stall characteristics of that aircraft have also been found [8], [9].

Equations (2.1)-(2.8) will be employed in the study of characteristics of the deep stall manoeuvre called Cobra.

### 3. The Law of the Aircraft Control

In order to perform a Cobra manoeuvre we need to control the angle of elevator deflection  $\delta_e$  and the thrust of power plant  $F$  of the aircraft.

#### 3.1. Method of Control of the Elevator Angle $\delta_e$

It is assumed that at the initial instant of time the aircraft is flying horizontally with a velocity  $V_0$  and the angle of elevator  $\delta_{e0}$ . The method of the elevator control which has been applied in this investigation is shown in Fig. 3.

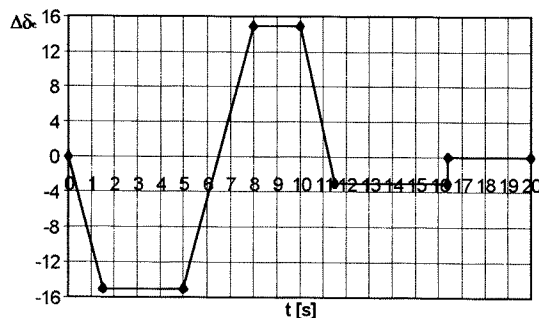


Fig. 3 The method of elevator control

At the beginning of the manoeuvre the elevator is moved from the position  $\delta_{e0}$  to  $\delta_{e0} - \Delta\delta_{e1}$  in a short time  $\Delta t_1$  and then it is held in this position until the elevation (pitch) angle of the aircraft achieves the value  $\Theta = 40^\circ$ . Next the elevator is moved in the time  $\Delta t_2 = 2\Delta t_1$  to the position  $\delta_{e0} + \Delta\delta_{e1}$  and subsequently it is held until the elevation angle reaches the value  $\Theta = 75^\circ$ . Now the angle of elevator is decreased in the time  $\Delta t_1$  to the position  $\delta_{e0} - \Delta\delta_{e2}$ . At the end of the manoeuvre,

for time  $t_k$ , the elevator is shifted to the initial position  $\delta_{e0}$ .

#### 3.2. Method of Control of the Thrust $F$

Cobra is an aircraft manoeuvre which should be performed without any appreciable change in altitude of flight. In this connection the thrust of power plant necessary for this manoeuvre can be determined from condition of forces equilibrium in the vertical direction. It is also assumed that the required thrust depends on the difference of angles  $(\Theta - \alpha)$  and the velocity of flow. Finally the law of thrust control can be written in the form

$$F(t) = F_0 \left\{ 1 - \tan[n(\Theta - \alpha)] \right\} \frac{V_0 - V}{V_{ref}} \quad (3.1)$$

where  $F_0$  is determined from the equilibrium condition of forces in the vertical direction

$$F_0 = [ng + P_{zs} \sin(\Theta - \alpha) - P_{zs} \cos(\Theta - \alpha)] / \sin\Theta \quad (3.2)$$

The thrust can also fulfil the inequality

$$F_{idle} \leq F(t) \leq F_{max} \quad (3.3)$$

where  $F_{idle}$  is the thrust of idle running and  $F_{max}$  is maximum thrust of power plant.

At the end of the manoeuvre, for  $t = t_k$ , the thrust necessary for the steady horizontal flight with the velocity  $V = V_0$  is assumed.

### 4. Numerical Analysis of Cobra Manoeuvres

A number of calculations have been carried out in order to investigate the course of flight parameters during Cobra manoeuvres.

Initial velocity has been assumed from  $V_0 = 100$  m/s to 180 m/s.

Cobra manoeuvres in longitudinal motion of the aircraft have been considered and next spatial motion manoeuvres have been studied taking into account gyroscopic coupling between longitudinal and lateral motions.

#### 4.1. Cobra Manoeuvre in Longitudinal Motion

Some results of numerical analysis will be presented for  $V_0 = 170$  m/s. For these calculations it is assumed  $\Delta\delta_{e1} = 25.37^\circ$ ;  $\Delta\delta_{e2} = 3^\circ$ ;  $\Delta t_1 = 1.5$  s and in Eq.(3.1)  $n = 4$ .  $V_{ref} = V_0 - 50$ . Results of numerical analysis are presented in Figs. 4-10.

From these figures it is seen that the aircraft is braked suddenly (Fig.4) and after 7.35 s its velocity decreases to 35.7 m/s, subsequently the velocity is growing up. The angle of attack  $\alpha$  is growing quickly (Fig.5) and it attains its maximum  $82.2^\circ$  at  $t = 4.3$  s. The rate of pitch  $q$

(Fig.6) and the angle of pitch  $\theta$  (Fig.7) also change rapidly. It should be mentioned that the maximum of  $\theta$  is  $123.1^\circ$  for 4.9s. From Fig.8 it is seen that there appears also a strong and short overload  $n_z=5.4$  for  $t=1.5$ s. Control of the elevator and the thrust control for this manoeuvre is shown in Figs. 9 and 10.

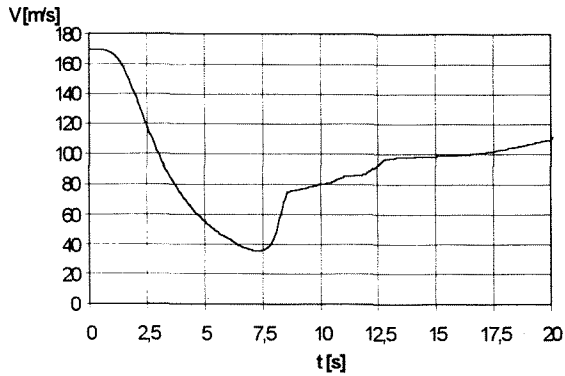


Fig.4 Course of velocity  $V$

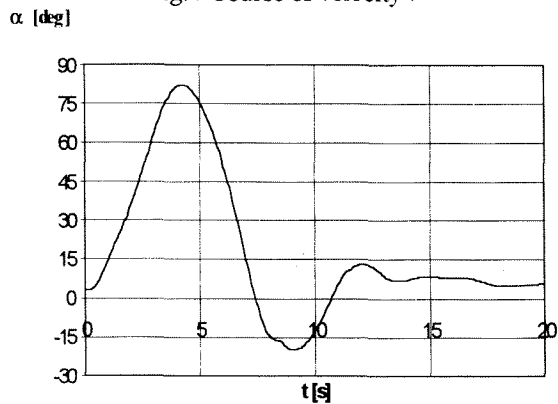


Fig.5 Course of angle of attack  $\alpha$

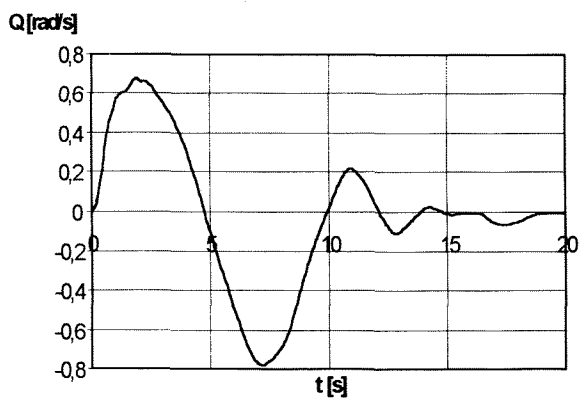


Fig.6 Course of pitch rate  $q$

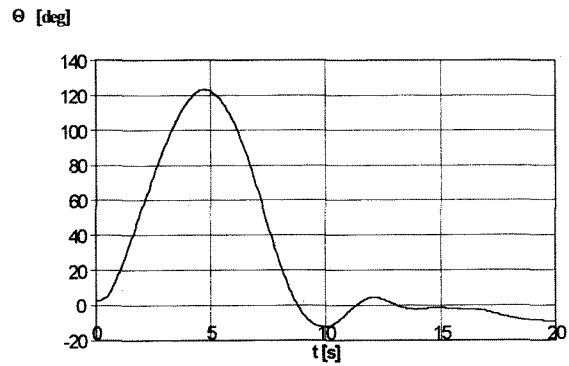


Fig.7 Course of angle of pitch  $\theta$

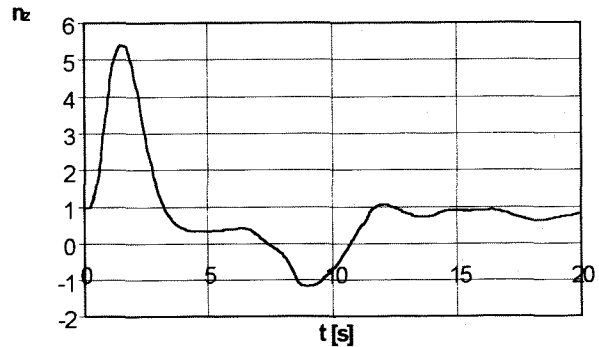


Fig.8 Course of overload coefficient  $n_z$

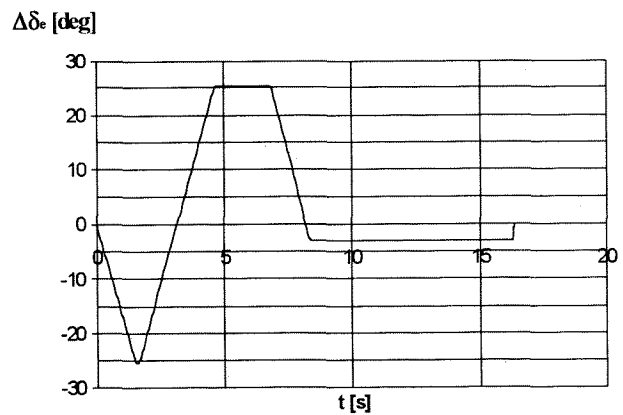


Fig.9 Elevator control for  $V_0=170$ m/s

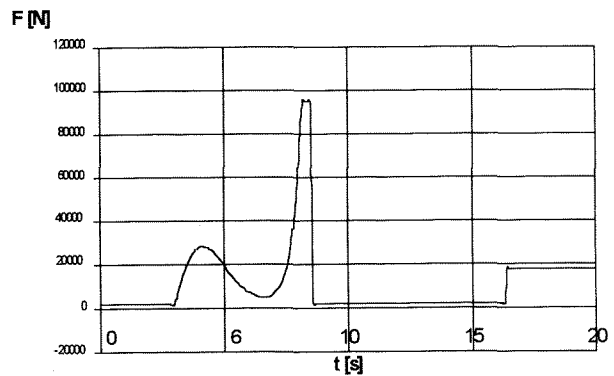


Fig.10 Thrust control for  $V_0=170$ m/s

The courses of flight parameters shown in Figs. 4-10 have been obtained for actual initial conditions. For other initial conditions the courses of those parameters can be different, however their character may be similar one if the initial conditions are suitably chosen.

#### 4.2. Cobra Manoeuvre in Spatial Motion

It is assumed that in the equations of motion (2.2) gyroscopic moment of rotating masses of the power plant is taken into account, which can couple longitudinal and lateral motions of the aircraft.

Some results of numerical analysis will be presented for the two values of initial velocity  $V_{01}=100\text{m/s}$  and  $V_{02}=170\text{m/s}$  and deflection of elevator  $\Delta\delta_{e11} = 14.8^\circ$ ,  $\Delta\delta_{e12} = 25.3^\circ$ .

For both values of initial velocity, two variants of calculations have been performed - that is neglecting the couplings between longitudinal and lateral motions - variants 10 and 20 and taking into account that couplings - variants 11 and 21.

Results of numerical analysis are presented in Figs. 11-24. In these figures courses of flight parameters are shown for four variants of solution of the problem.

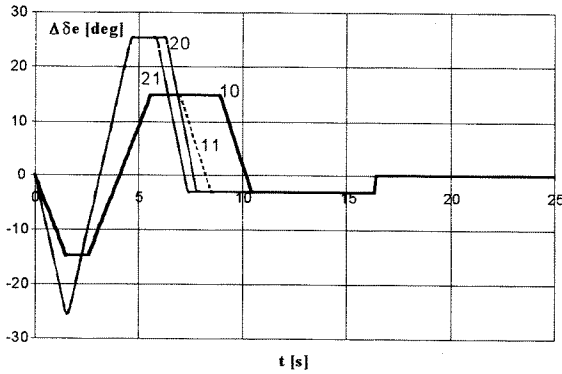


Fig. 11 Control of elevator angle  $\Delta\delta_e$

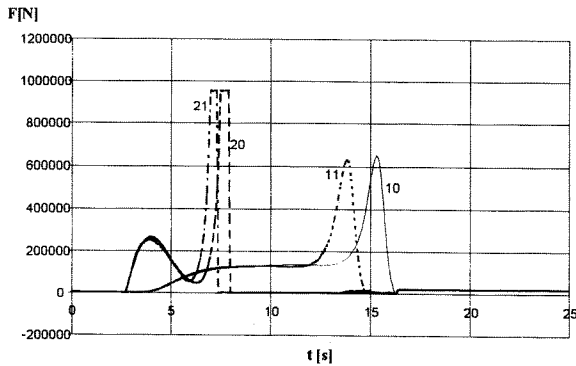


Fig. 12 Control of the thrust  $F$

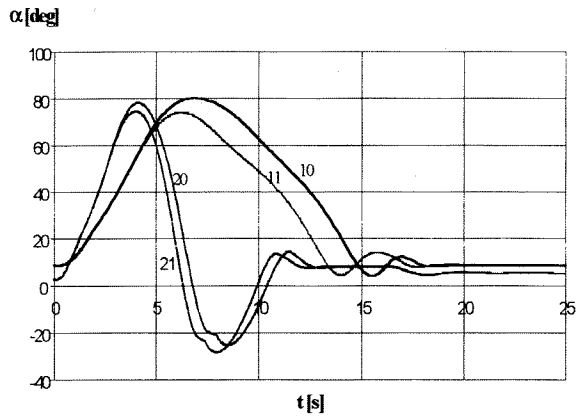


Fig. 13 Course of angle of attack  $\alpha$

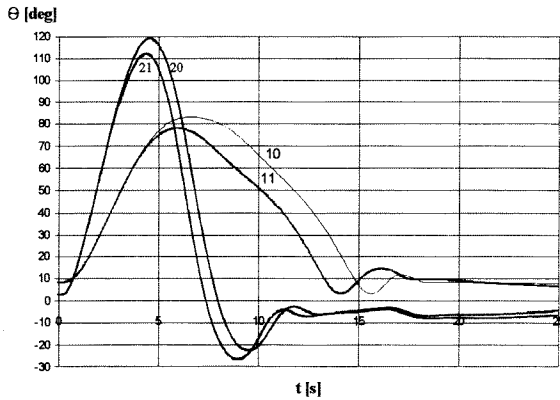


Fig. 14 Course of angle of pitch  $\Theta$

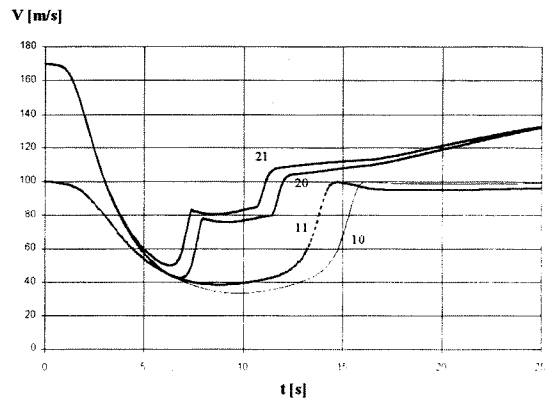


Fig. 15 Course of velocity  $V$

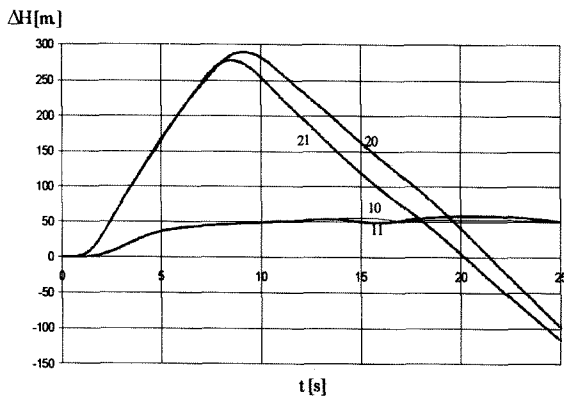


Fig. 16 Change of altitude  $\Delta H$

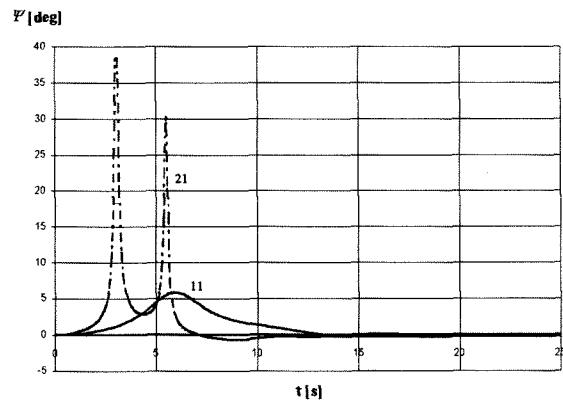


Fig. 20 Course of yawing angle  $\Psi$

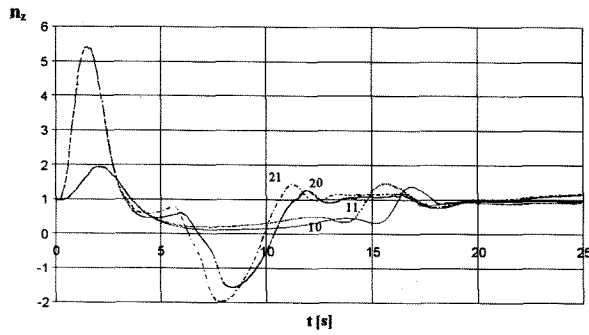


Fig. 17 Course of overload coefficient  $n_z$

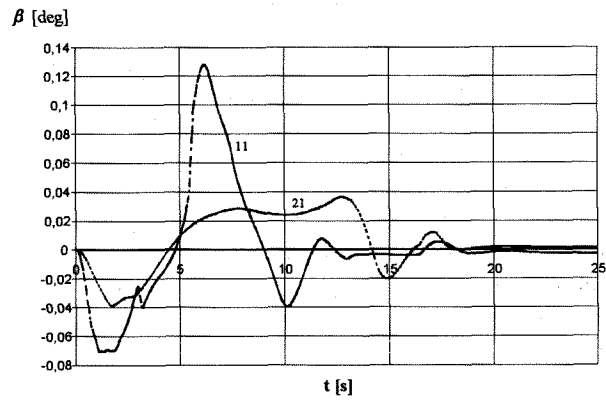


Fig. 21 Course of sideslip angle  $\beta$

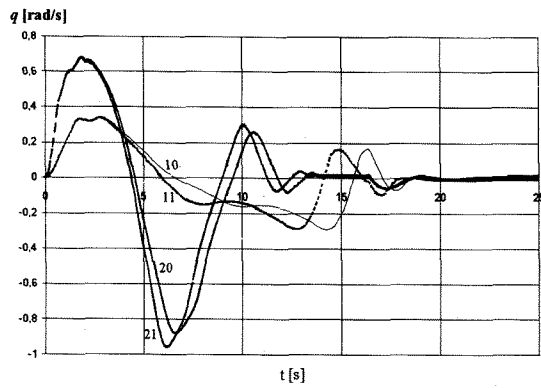


Fig. 18 Course of pitch rate  $q$

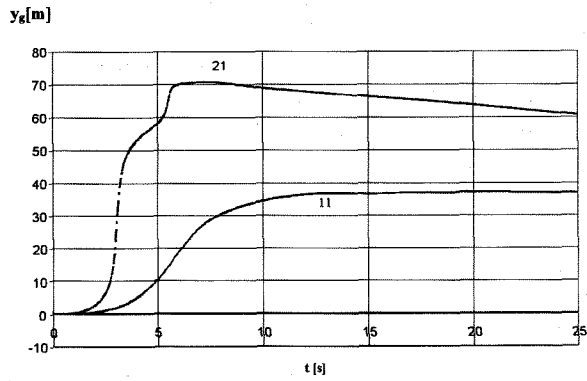


Fig. 22 Course of lateral deflection  $y_g$

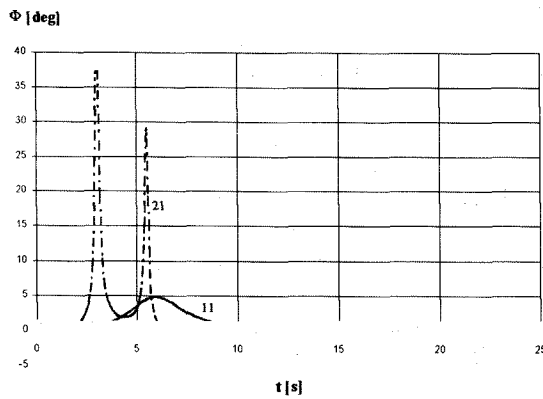


Fig. 19 Course of rolling angle  $\Phi$

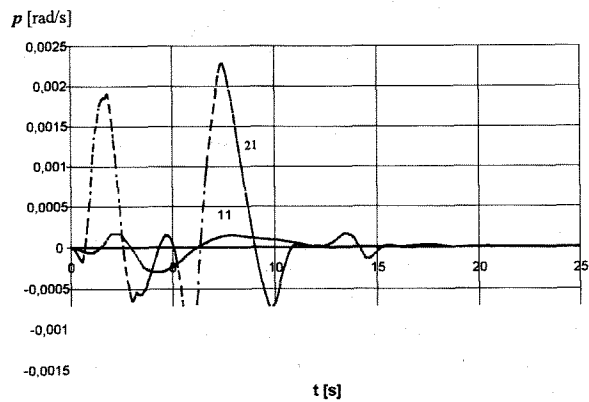


Fig. 23 Course of rolling rate  $p$

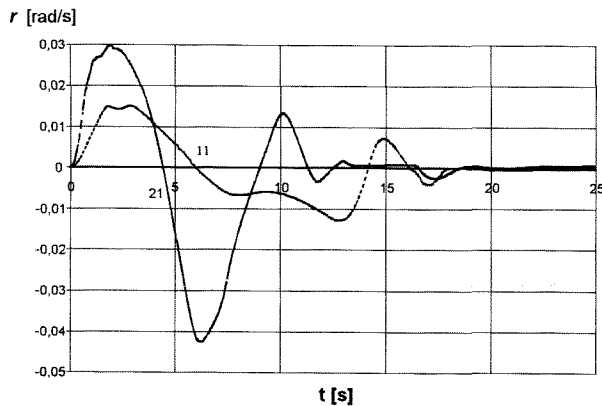


Fig.24 Course of yawing rate  $r$

From these figures it is seen that after taking into account the couplings between the longitudinal and lateral motions there appear not only lateral deflections of the motion but also a change of the parameters in longitudinal motion.

The method of control of the elevator  $\delta_e$  and the thrust of power plant  $F$  is shown in Figs. 11 and 12. It is seen that duration of manoeuvre is shortened after taking into account the coupling of motions.

The course of change of the angle of attack  $\alpha$  is shown in Fig. 13, the angle of pitch  $\theta$  - in Fig.14 and the velocity of flight  $V$  - in Fig.15.

It is seen from these figures that during the manoeuvre the angle of attack and pitch increase suddenly and the velocity decreases. Maximum values of  $\alpha$ ,  $\theta$  and minimum of  $V$  are given in table 1. There are also included maximum values of the change of altitude  $\Delta H$  from Fig.16 and overload coefficient  $n_z$  from Fig.17.

Table 1

variants of calc.	10	11	20	21
$\alpha_{max}$	80.23	73.99	78.16	74.6
$\theta_{max}$	83.35	78.25	119.08	112.10
$V_{min}$	33.46	38.40	42.35	50.08
$\Delta H_{max}$	56.21	53.36	289.47	277.52
$n_{zmax}$	1.94	1.94	5.41	5.41

We can see that  $\alpha_{max}$  exceeds  $80^\circ$  for the variant 10 only. The angles  $\theta_{max}$  are close to  $\alpha_{max}$  for the variants 10 and 11, while for variants 20 and 21 they exceed  $110^\circ$ . After taking into account the coupling of motions the maximum value of  $V$  increases.

Taking into account the method of control proposed in this paper, we obtain a change in altitude during the Cobra manoeuvres, which does not exceed 60m for variants 10, 11 and is about 300m for variants 20, 21.

Maximum coefficients of overload  $n_z$  do not depend on the coupling of motions and they increase with the value of initial velocity  $V_0$ . The courses of pitch velocity  $q$  are shown in Fig.18. They depend on the value of initial velocity  $V_0$  and the coupling of motions. In the next Figs. 19-24 courses of lateral parameter of the aircraft motion during Cobra manoeuvres are presented if the couplings of motions is taken into account.

It can be seen from these figures that the courses of the parameters depend on the value of initial velocity  $V_0$  and all the angular parameters decay after ending the manoeuvre, however the lateral deflection of the aircraft trajectory remains different from zero (Fig.22).

The conclusion resulting from this analysis is that in order to perform a Cobra manoeuvre for a given value of the of initial velocity  $V_0$ , a properly chosen deflection of the elevator  $\Delta\delta_{e1}$  is necessary, what is shown, by way of example, in Fig.25. For greater values  $\Delta\delta_{e1}$  the aircraft is going to make a loop and for smaller values  $\Delta\delta_{e1}$  there is a hump.

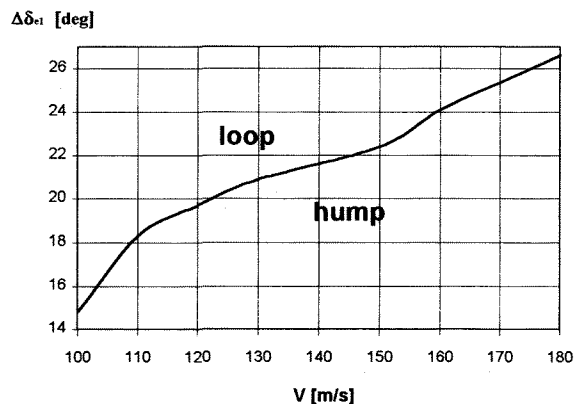


Fig.25 Optimum deflections of elevator  $\Delta\delta_{e1}$  for Cobra manoeuvres

#### References

1. Pennington T., Kotarba R., F16N Supersonic Adversary Aircraft Evaluation, 19-th Annual Symposium of Society of Flight Test Engineers, Proceedings, Arlington, Texas, USA, 14-18.08. 1988.
2. Medina M., Shahaf M., Post Stall Characteristics of Highly Augmented Fighter Aircraft, 17-th Congress of ICAS, Proceedings, Stockholm, Sweden, 9-14.09. 1990.
3. Wanstall B., Wilson J.R., Air Combat beyond the Stall, Interavia Aerospace Review, No 5, 1990.
4. Orlik-Ruckemann K.J., Aerodynamics of Manoeuvring Aircraft, Canadian Aeronautics and Space Journal, v.38, No 3, 1992.
5. Etkin B., Dynamics of Atmospheric Flight, Ed. John Wiley, New York, London, Sydney, Toronto, 1972.

6. Bekey G.A., Karplus W.J., Hybrid Computation, Ed. John Wiley, New York, 1968.
7. Dźygadło Z., Sibilski K., Dynamics of Spatial Motion of an Aeroplane After Drop of Loads, Journal of Technical Physics, v. 29, No 3-4, Warsaw, 1988.
8. Whitford R., Design for Air Combat, Ed. Jane's Information Group, London, 1989.
9. Ghmmam A.H.A., Goraj Z., Review of the Influence of High Angle of Attack Aerodynamics on Aircraft Dynamic Stability, Journal of Theoretical and Applied Mechanics, v. 33, No 3, 1995.
10. Sibilski K., Modeling of Aeroplane Dynamics in Extreme Flight Conditions, 20-th Congress of ICAS, Sorrento, Italy, 1996.